Learning & Nonlinear Models (L&NLM) – Journal of the Brazilian Neural Network Society, Vol. 8, Iss. 1, pp. 23-40, 2010

Nonholonomic Mobile Robot with Kinematic Disturbances in the Trajectory Tracking: A Variable Structure Controller

Nardênio A. Martins, Ebrahim S. Elyoussef, Douglas W. Bertol, Edson R. De Pieri, Ubirajara F. Moreno, Eugênio B. Castelan

DAS-CTC-UFSC, Caixa Postal 476, CEP 88040-900 - Florianópolis SC
{nardenio, ebrahim,, dwbertol, edson, moreno, eugenio}@das.ufsc.br

Abstract - In this paper, a trajectory tracking control for a nonholonomic mobile robot subjected to kinematic disturbances is proposed. A variable structure controller based on the sliding mode theory is used, and applied to compensate these disturbances. To minimize the problems found in practical implementations of the classical variable structure controllers, and eliminate the chattering phenomenon a neural compensator is used, which is nonlinear and continuous, in lieu of the discontinuous portion of the control signals present in classical forms. The proposed neural compensator is designed by the Gaussian radial basis function neural networks modeling technique and does not require the time-consuming training process. Stability analysis is guaranteed based on the Lyapunov method. Simulation results are provided to show the effectiveness of the proposed approach.

Keywords: Mobile robot, trajectory tracking, variable structure control, sliding mode theory, neural networks, Lyapunov method.

1 INTRODUCTION

The wheeled mobile robot of the type (2,0) is plenty used in the literature as test platform, due to its mechanical simplicity, and for represent adequately the challenges of the control problem treated in this paper [Campion and Chung, 2008; Morin and Samson, 2008]. Thus, this paper describes the design of a kinematic controller, for this type of mobile robot, based on the sliding mode theory, considering the presence of kinematic disturbances.

Variable structure control design utilizes a high speed switching control law to drive the nonlinear predefined states trajectories onto a specified surface (called the sliding or switching surface), to attain the conventional goals of control such as stabilization and tracking.

Due to robustness properties against uncertainties, modeling imprecision and disturbances, the VSC has become very popular and used in many application areas [Utkin et al., 2009; Decarlo et al., 1996; Hung et al., 1993; Gao and Hung, 1993]. However, this control scheme has important drawbacks that limit its practical applicability, such as high frequency switching (chattering) and large authority control, which deteriorate the system performance [Shuwen et al., 2000]. The first drawback mentioned is due to control actions that are discontinuous on the sliding surfaces, which causes the high frequency switching in a boundary of the sliding surfaces. This high frequency switching might excite unmodeled dynamics and impose undue wear on the actuators, so that the control law would not be considered acceptable. The second drawback mentioned, is based on the requirement of a priori knowledge of the boundary of uncertainty in compensators. If boundary is unknown, a large value has to be applied to the gain of discontinuous part of control signal and this large control gain may intensify the high frequency switching on the sliding surfaces.

Researches have been developed using softcomputing methodologies, such as artificial neural networks, in order to improve the performance and reduce the problem found in practical implementations of variable structure controllers as mentioned in [Efe and Kaynak, 2001; Kaynak et al., 2001]. In this paper, the radial basis function neural networks (RBFNNs) are applied to avoid the chattering and compensate the kinematic disturbances, since the structure of an RFBNN is simpler than a multi-layer perceptron (MLP), the learning rate of a RBFNN is generally faster than a MLP, and a RBFNN is easily mathematically tractable [Seshagiri and Khalil, 2000].

Unlike other works that use the sliding mode theory applied to mobile robots [Elyoussef et al., 2010; Li et al., 2009; Lee et al., 2009; Defoort et al., 2007; Chwa, 2004; Chwa, 2002; Yang and Kim, 1999; Yang and Kim, 1999a; Shim et al., 1995; Guldner and Utkin, 1994], the contributions of this paper are:

- A variable structure controller (VSC) in Cartesian coordinates to compensate the kinematic disturbances, based on the sliding mode theory;
- A neural compensator (NC) used to replace the discontinuous portion of the classical VSC, avoiding the chattering as well as suppressing the kinematic disturbances without having any prior knowledge of their boundary;

- The implementation of the NC is based on the partitioning of the RBFNNs into several smaller subnets in order to obtain a more efficient computation;
- The weights of the hidden layer of RBFNNs are updated online to ensure the stability of the overall system;
- The stability analysis of the mobile robot control system, and of the learning algorithm are proved using the Lyapunov theory.

This paper is organized as follows. The section 2 presents the kinematic model for nonholonomic mobile robots with disturbances, and the corresponding error dynamics. The proposed VSC and a VSC with NC for a reference trajectory tracking is described in the section 3. The section 4 shows the simulation results, and the section 5 presents the conclusions.

2 PROBLEM FORMULATION

In this section the kinematic model, the trajectory tracking control problem, and the error dynamics for a nonholonomic mobile robot are described.

2.1 Kinematics of a Mobile Robot

A typical example of a nonholonomic mobile robot is shown in Figure 1. The mobile robot has two driving wheels mounted on the same axis and a free front wheel. The two driving wheels are independently driven by two actuators to achieve the motion and orientation. The position of the mobile robot in the Cartesian inertial frame $\{X_o, O, Y_o\}$ can be described by a vector $\overrightarrow{OC}$, and the orientation θ between the mobile robot base frame $\{X_c, C, Y_c\}$ and the Cartesian inertial frame, where C is the center of mass coordinates (guidance point), with P, d, r, and $2R$ being the intersection of the axis of symmetry with the driven wheel axis, the distance from the point C to the point , the radius of the wheels, and the distance between the driven wheels, respectively.

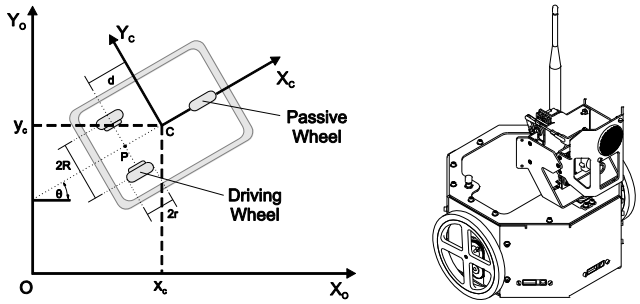

Figure 1: Nonholonomic mobile robot and coordinate systems.

The posture vector $q \in \Re^3$ of the mobile robot is described by three generalized coordinates as:

$$q = [x_c, y_c, \theta] \tag{1}$$

where (x_c, y_c) are the coordinates of C.

Under the condition of pure rolling and non-slipping, and considering $d = 0$, the kinematic model of the mobile robot can be expressed as:

$$\dot{q} = S(q)v(t) \tag{2}$$

with:

$$S(q) = \begin{bmatrix} \cos(\theta) & 0 \\ \sin(\theta) & 0 \\ 0 & 1 \end{bmatrix} \tag{3}$$

and $v(t) = [v_l \quad \omega_a]^T$ representing the linear and angular velocities of the mobile robot in point *C*, respectively. However such kinematic model, equation (3), does not take into account the measurement noise, modeling uncertainties and disturbances. As there are input disturbances, a more realistic kinematic model of the mobile robot can addressed by:

$$\dot{q} = S(q)\ v(t) + d_v(t) \tag{4}$$

where $d_v(t)$ represents the unknown disturbances only, which are assumed to be upper bounded by:

$$| d_v | < \varepsilon_v \tag{5}$$

with ε_v being positive bounded constant. Thus, the kinematic model of a mobile robot, equation (4), may be subject to the so-called matched disturbance, which is given as follows [Canudas de Wit and Khennouf, 1995]:

$$d_v(t) = [\rho_M(t) \quad 0]^T \tag{6}$$

where $\rho_M(t)$ denotes a bounded disturbance. From a control point of view, it is easy to see from equations (4) and (6) that the matched disturbance problem is a special case of the kinematic model used in equation (4). It is important to emphasize that also there are input disturbances in v_l and ω_a simultaneously, which represents a more realistic kinematic model of the mobile robot, as can be found in [Martins and De Pieri, 2010].

2.2 Error Dynamics of a Mobile Robot

In order to formulate the trajectory tracking problem, a reference trajectory is generated by the following reference kinematic model:

$$\dot{q}_r = S(q_r)v_r, \qquad \dot{x}_r = v_{l_r}\cos(\theta_r), \qquad \dot{y}_r = v_{l_r}\sin(\theta_r), \qquad \dot{\theta}_r = \omega_{a_r} \tag{7}$$

where $q_r = [x_r \quad y_r \quad \theta_r]^T \in \Re^3$ denotes the reference posture of the mobile robot, the structure of $S(q_r)$ is defined as in equation (3), and $v_r = [v_{l_r} \quad \omega_{a_r}]^T$ denotes the reference linear and angular velocities of the mobile robot, respectively. With regard to equation (7), is assumed that the signal $v_r(t)$ is chosen to produce the desired motion and that $v_r(t)$, $\dot{v}_r(t)$, $q_r(t)$, and $\dot{q}_r(t)$ are bounded for all time.

The trajectory tracking control problem of a mobile robot is solved designing a control input $v(t) = [v_l \quad \omega_a]^T$ such that the system, equation (4), follows the reference, equation (7), despite of disturbances. In fact, the aim is to converge the tracking errors ($e_x = x_r - x_c$, $e_y = y_r - y_c$, $e_\theta = \theta_r - \theta$) to zero, respecting the following constraints:

$$|v_l| \le v_{l_{\max}}, \quad |\omega_a| \le \omega_{a_{\max}} \tag{8}$$

Converting the tracking errors in the inertial frame to the mobile robot frame, the posture error equation of the mobile robot can be denoted as:

$$\tilde{z} = \begin{bmatrix} \tilde{x} \\ \tilde{y} \\ \tilde{\theta} \end{bmatrix} = \begin{bmatrix} \cos(\theta) & \sin(\theta) & 0 \\ -\sin(\theta) & \cos(\theta) & 0 \\ 0 & 0 & 1 \end{bmatrix} \begin{bmatrix} e_x \\ e_y \\ e_\theta \end{bmatrix} \tag{9}$$

The error dynamics can be obtained from the time derivative of equation (9) as:

$$\dot{\tilde{z}} = \begin{bmatrix} \dot{\tilde{x}} \\ \dot{\tilde{y}} \\ \dot{\tilde{\theta}} \end{bmatrix} = \begin{bmatrix} v_{l_r} \cos(\tilde{\theta}) \\ v_{l_r} \sin(\tilde{\theta}) \\ \omega_{a_r} \end{bmatrix} + \begin{bmatrix} -1 & \tilde{y} \\ 0 & -\tilde{x} \\ 0 & -1 \end{bmatrix} \begin{bmatrix} v_l + \rho_M \\ \\ \omega_a \end{bmatrix} \tag{10}$$

by using equation (6).

3 CONTROL DESIGN FOR THE TRAJECTORY TRACKING

In this section, a VSC is designed for the kinematic model with disturbances only, equation (4). The RBFNNs are used as replacement for the discontinuous portion of the classical VSC to avoid the chattering as well as to suppress the kinematics disturbances. For such development is required the selection of the sliding surfaces and a brief description of the generic modeling of nonlinear systems to the VSC design [Utkin et al., 2009; Hung et al., 1993; Gao and Hung, 1993].

3.1 Choice of Sliding Surfaces

The VSC is a feedback control with high-speed switching, whose action takes place in two phases: the reaching phase and the sliding phase. In the reaching phase, the states trajectories of the system (linear or nonlinear) are lead to a place in the states space chosen by the designer. In general, this place is defined by linear surfaces of the control errors ($\tilde{z} = [\tilde{x} \quad \tilde{y} \quad \tilde{\theta}]^T$), known as switching or sliding surfaces (σ), each one of them described by:

$$\sigma_i(\tilde{z}, t) = c_i^T \tilde{z}_i = 0, \quad i = 1,2 \tag{11}$$

In the sliding phase, the states trajectories are forced to remain on the sliding surfaces. By choosing appropriately the constants c_i^T of equation (11), the errors will tend exponentially to zero according to the standard determined by these constants, during the sliding phase.

Thus, to control the kinematic model, equation (4), are selected the following sliding surfaces:

$$\sigma(\tilde{z}, t) = \begin{bmatrix} \sigma_1 \\ \sigma_2 \end{bmatrix} = \begin{bmatrix} k_1 \tilde{x} \\ k_2 \tilde{y} + k_3 \tilde{\theta} \end{bmatrix} \tag{12}$$

where k_1, k_2, k_3 are positive constants. To each control input is associated one sliding surface σ_i, $i = 1,2$.

3.2 Generic Model for Nonlinear Systems

The derivation of the VSC and their properties are made directly for an important class of nonlinear systems, whose model, in the form of state equations, is given by:

$$\dot{\tilde{z}}(t) = A(\tilde{z}, \rho, t) + B(\tilde{z}, \rho, t) v(\tilde{z}, t) + d_b(t) \tag{13}$$

with $A(\tilde{z}, \rho, t) = A_0(\tilde{z}, t) + \Delta A(\tilde{z}, \rho, t)$ and $B(\tilde{z}, \rho, t) = B_0(\tilde{z}, t) + \Delta B(\tilde{z}, \rho, t)$, where $\tilde{z}(t)$ is the vector of states; $A(\tilde{z}, \rho, t)$ is the vector of nonlinear functions; $v(\tilde{z}, t)$ is the vector of control inputs; $\rho(\tilde{z}, t)$ is the vector of parametric uncertainties; $B(\tilde{z}, \rho, t)$ is the matrix of nonlinear functions; $\Delta A(\tilde{z}, \rho, t)$ and $\Delta B(\tilde{z}, \rho, t)$ are the vector and the matrix representing the disturbances in the system arising from the parametric uncertainties, respectively; $d_b(t)$ is the vector of external disturbances; and $A_0(\tilde{z}, t)$, $B_0(\tilde{z}, t)$ refers to the vector and the matrix of nominal parameters, respectively.

The aim of this study is the derivation of a VSC robust to the present disturbances in the kinematic model, equation (4). To ensure the robustness of the controller, the disturbances should be bounded, the matrix $B(\tilde{z}, \rho, t)$ should be nonsingular and the following matching conditions must be satisfied:

$$\Delta A(\tilde{z}, \rho, t) = B_0(\tilde{z}, t) \tilde{a}$$

$$\Delta B(\tilde{z},\rho,t) = B_0(\tilde{z},t)\tilde{b}$$
$$d_b(t) = B_0(\tilde{z},t)\tilde{d}_0 \tag{14}$$

which means that $\Delta A(\tilde{z},\rho,t)$, $\Delta B(\tilde{z},\rho,t)$, and $d_b(t)$ must belong to the image of $B_0(\tilde{z},t)$; $\tilde{a}$ and $\tilde{b}$ are the vector and the matrix that incorporate the parametric uncertainties, respectively; and $\tilde{d}_0$ represents the external disturbances.

So, the error dynamics, equation (10), can be rewritten based in equations (13) and (14) as:

$$\dot{\tilde{z}} = A_0(\tilde{z},t) + B_0(\tilde{z},t)v(\tilde{z},t) + d_b(t) \tag{15}$$

since there are not parametric uncertainties ($\Delta A = 0$, $\Delta B = 0$), and $d_b(t)$ is defined as:

$$d_b(t) = B_0(\tilde{z},t)d_v(t) \tag{16}$$

for the case of matched disturbance, equation (10).

3.3 Variable Structure Control Design

In order to have influences also on the process of reaching of the sliding surfaces, the control $v(\tilde{z},t)$ will be chosen in such a way to impose $\sigma(\tilde{z},t)$ to have the dynamics given by the following first order differential equation:

$$\dot{\sigma}(\tilde{z},t) = -Gsign(\sigma) - K_p h(\sigma) \tag{17}$$

where G = diag{G_{11}, G_{22}} and K_p = diag{Kp_{11}, Kp_{22}}, $h(\sigma) = \sigma$ (could be another function, since that $\sigma^T h(\sigma) > 0$), and $sign(\sigma) = \dfrac{\sigma}{|\sigma|}$ is a discontinuous function.

Rewriting the equation (17) for the *i-th* sliding surface, one obtains:

$$\dot{\sigma}_i(\tilde{z},t) + k_{pi}\sigma_i = -g_i sign(\sigma_i) \tag{18}$$

Returning to equation (17) and taking into account the equation (15), results in:

$$\dot{\sigma}(\tilde{z},t) = \frac{\partial\sigma(\tilde{z},t)}{\partial\tilde{z}}\dot{\tilde{z}} + \frac{\partial\sigma(\tilde{z},t)}{\partial t} = \frac{\partial\sigma}{\partial\tilde{z}}(A_0 + B_0 v + d_b) + \frac{\partial\sigma}{\partial t} = \frac{\partial\sigma}{\partial\tilde{z}}(A_0 + B_0 v) + \frac{\partial\sigma}{\partial\tilde{z}}d_b + \frac{\partial\sigma}{\partial t} \tag{19}$$

with

$$\frac{\partial\sigma(\tilde{z},t)}{\partial\tilde{z}} = \begin{bmatrix} k_1 & 0 & 0 \\ 0 & k_2 & k_3 \end{bmatrix} \tag{20}$$

whence is derived the following control law:

$$v = -B_{0_\sigma}^{-1}\left(A_{0_\sigma} + \frac{\partial\sigma}{\partial t} + Gsign(\sigma) + K_p\sigma \right) \tag{21}$$

in which

$$A_{0_\sigma} = \frac{\partial \sigma}{\partial \tilde{z}} A_0 = \begin{bmatrix} k_1 v_{l_r} \cos(\tilde{\theta}) \\ k_2 v_{l_r} \sin(\tilde{\theta}) + k_3 \omega_{a_r} \end{bmatrix} \tag{22}$$

$$B_{0_\sigma} = \frac{\partial \sigma}{\partial \tilde{z}} B_0 = \begin{bmatrix} -k_1 & k_1 \tilde{y} \\ 0 & -k_2 \tilde{x} - k_3 \end{bmatrix} \tag{23}$$

$$B_{0_\sigma}^{-1} = \begin{bmatrix} -\frac{1}{k_1} & -\frac{\tilde{y}}{k_2 \tilde{x} + k_3} \\ 0 & -\frac{1}{k_2 \tilde{x} + k_3} \end{bmatrix} \tag{24}$$

and $k_2 = k_3 \alpha$, $0 \le \alpha \le \frac{1}{\|\tilde{x}\| + 1}$.

Defining

$$v^* = - \, Gsign(\sigma) + K_p \sigma \tag{25}$$

and replacing the equation (21) in equation (19), results in:

$$\dot{\sigma} = A_{0_\sigma} - B_{0_\sigma} B_{0_\sigma}^{-1} \left(A_{0_\sigma} + \frac{\partial \sigma}{\partial t} - v^* \right) + d_\sigma + \frac{\partial \sigma}{\partial t} = -Gsign(\sigma) - K_p \sigma + \psi \tag{26}$$

where of equation (16) one obtains:

$$d_\sigma = \frac{\partial \sigma}{\partial \tilde{z}} d_b \tag{27}$$

$B_{0_\sigma} B_{0_\sigma}^{-1} = I_n$, and $\psi = d_\sigma$ are the disturbances in the system.

3.4 Stability Analysis

Choosing $V = \frac{1}{2} \sigma^T \sigma$ as a Lyapunov function candidate, which is positive definite, the sliding surface will be attractive since the control law, equation (21), ensures that $\dot{V} = \sigma^T \dot{\sigma}$ is negative definite. Using the result described by equation (26), an expression for $\dot{V}$ is immediately obtained, that is,

$$\dot{V} = \sigma^T \dot{\sigma} = -\sigma^T Gsign(\sigma) - \sigma^T K_p \sigma + \sigma^T \psi \tag{28}$$

As $\sigma^T K_p \sigma \ge 0$, the condition $\dot{V} \le 0$ can be expressed by:

$$\sigma^T Gsign(\sigma) \ge \sigma^T \psi \tag{29}$$

which is satisfied if the diagonal elements of *G* meet the following restriction:

$$g_i > |\bar{\psi}_i|, \ \forall i \tag{30}$$

If $g_i > \bar{\psi}_i$, then $\dot{V} \leq 0$ ($\dot{V} = 0$ only when $V = 0$), which implies that V may decrease to $V = 0$ exponentially; however, if $g_i < \bar{\psi}_i$, there is a value of $V = V_{ss} > 0$ for which $\dot{V} = 0$ can leading to nonzero errors. Therefore, it is possible to affirm that if the disturbances are better estimated, the results will be better.

However, for the existence and reachability of a sliding mode it is enough to select a $V > 0$, so that the sliding surface will be attractive since the control law, equation (21), ensures that $\dot{V} < 0$. For this, in the derivation of equation (21), it is necessary that matrix B_{0_σ} is non-singular. As G is positive definite diagonal matrix in equation (21), then the sliding mode can be enforced under the condition that the matrix B_{0_σ} is positive definite and elements of the matrix G are large enough. But, in this control law, equation (21), the matrix B_{0_σ} is non-singular only. To solve this problem, a diagonalization method is used, which is based on the fact that the equivalent system is invariant to a non-singular sliding surface transformation, as verified in the Theorem 2 and their proof described in [DeCarlo, Zak and Matthews, 1988]. Loosely stated, Theorem 2 says that the motion in the sliding mode is independent of a non-singular possibly time varying transformation of the sliding surfaces, and that any non-singular transformation with bounded derivatives will produce the same equivalent system.

In particular, consider the new sliding surfaces as:

$$\bar{\sigma}(\tilde{z},t) = \Psi(\tilde{z},t)\sigma(\tilde{z},t) \tag{31}$$

for an adequate non-singular transformation $\Psi(\tilde{z},t) \in \Re^{m\times m}$, which is defined as:

$$\Psi(\tilde{z},t) = \left(\frac{\partial \sigma}{\partial \tilde{z}} B_0\right)^T = B_{0_\sigma}{}^T \tag{32}$$

Differentiating V, and replacing the equations (19) and (27), results in:

$$\dot{V} = \sigma^T \dot{\sigma} = \sigma^T \frac{\partial \sigma}{\partial \tilde{z}} A_0 + \sigma^T \frac{\partial \sigma}{\partial \tilde{z}} B_0 v + \sigma^T \frac{\partial \sigma}{\partial t} + \sigma^T \frac{\partial \sigma}{\partial \tilde{z}} B_0 d_v \tag{33}$$

and in the sequence, doing necessary algebraic manipulations and using equations (31) and (32), one obtains:

$$\begin{aligned} \dot{V} &= \sigma^T B_{0_\sigma} B_{0_\sigma}^{-1} A_{0_\sigma} + \sigma^T B_{0_\sigma} B_{0_\sigma}^{-1} \frac{\partial \sigma}{\partial t} + \sigma^T B_{0_\sigma} v + \sigma^T B_{0_\sigma} d_v \\ &= (B_{0_\sigma})^T \sigma^T B_{0_\sigma}^{-1} \left(A_{0_\sigma} + \frac{\partial \sigma}{\partial t}\right) + (B_{0_\sigma})^T \sigma^T v + d_v \\ &= \bar{\sigma}^T B_{0_\sigma}^{-1} \left(A_{0_\sigma} + \frac{\partial \sigma}{\partial t}\right) + \bar{\sigma}^T v + d_v \end{aligned} \tag{34}$$

Selecting control law v as:

$$v = -B_{0_\sigma}{}^{-1} \left(A_{0_\sigma} + \frac{\partial \sigma}{\partial t}\right) - G\,sign(\bar{\sigma}) + K_p \bar{\sigma} \tag{35}$$

Replacing equation (35) into equation (34), the $\dot{V}$ stays:

$$\dot{V} = -\bar{\sigma}^T G\,sign(\bar{\sigma}) + K_p \bar{\sigma} + \bar{\sigma}^T d_v \tag{36}$$

with $\bar{\sigma} = \begin{bmatrix} -k_1{}^2 \tilde{x} & k_1 \tilde{y} k_1 \tilde{x} - k_2 \tilde{x} + k_3 & k_2 \tilde{y} + k_3 \tilde{\theta} \end{bmatrix}^T$. The equation (36) is similar the equation (28), therefore, the same conclusions about the stability analysis, considering the equations (29) and (30), are valid. Moreover, sliding mode occurs in the manifold $\bar{\sigma}(\tilde{z},t) = 0$. The transformation, equations (31) and (32), is non-singular, therefore, the manifolds

$\sigma(\tilde{z},t)=0$ and $\bar{\sigma}(\tilde{z},t)=0$ coincide and sliding mode takes place in the manifold $\sigma(\tilde{z},t)=0$, which was selected to design sliding motion with the desired properties.

3.5 Neural Compensator Design

Due to delays, physical limitations of actuators and imperfections of switching, it is not possible to switch the control from a value to another instantaneously. Because of this, the states trajectory varies in a vicinity around the sliding surface, instead of sliding over it. This phenomenon, known as chattering, can be avoided or at least reduced using RBFNNs, which are nonlinear and continuous functions, to approximate $G\,\mathrm{sgn}(\bar{\sigma})$ in equation (35) [Martins et al., 2008]. Then v stays,

$$\begin{aligned} v &= -B_{0_\sigma}^{-1}\left(A_{0_\sigma}+\frac{\partial\sigma}{\partial t}\right)-\hat{P}(\bar{\sigma})-K_p\bar{\sigma} \\ &= -B_{0_\sigma}^{-1}\left(A_{0_\sigma}+\frac{\partial\sigma}{\partial t}\right)-\left[\ \hat{W}_{\bar{\sigma}}{}^{T}\bullet\ \xi_{\bar{\sigma}}(\bar{\sigma})\ \right]-K_p\bar{\sigma} \end{aligned} \tag{37}$$

where $\hat{W}_{\bar{\sigma}}$, $\xi_{\bar{\sigma}}(\bar{\sigma})$ are Ge-Lee (GL) vectors [Ge, 1996], and their respective elements are $\hat{W}_{\bar{\sigma}_k}$, and $\xi_{\bar{\sigma}_k}(\bar{\sigma})$; with $\hat{P}(\bar{\sigma})$ being an $n\times 1$ output vector of the RBFNNs. The stability of the RBFNNs can be analyzed, using GL matrix and vector [Ge, 1996], which are defined by {.}, and by its product operator '•'. The ordinary matrix and vector are denoted by [.].

Thus, one can choose the Lyapunov function candidate as follows:

$$V=\frac{1}{2}\left(\sigma^T\sigma+\sum_{k=1}^{n}\tilde{W}_{\bar{\sigma}_k}{}^{T}\Gamma_{\bar{\sigma}_k}{}^{-1}\tilde{W}_{\bar{\sigma}_k}\right) \tag{38}$$

where $\Gamma_{\bar{\sigma}_k}$ is a dimensional compatible symmetric positive definite matrix, and $\tilde{W}_{\bar{\sigma}_k} = W_{\bar{\sigma}_k} - \hat{W}_{\bar{\sigma}_k}$.

Differentiating equation (38), making the necessary mathematical manipulations, and replacing equation (37), $\dot{V}$ is obtained as:

$$\dot{V}=-\bar{\sigma}^T\left[\ \hat{W}_{\bar{\sigma}}{}^{T}\bullet\ \xi_{\bar{\sigma}}(\bar{\sigma})\ \right]-\bar{\sigma}^TK_p\bar{\sigma}+\bar{\sigma}^Td_v-\sum_{k=1}^{n}\tilde{W}_{\bar{\sigma}_k}{}^{T}\Gamma_{\bar{\sigma}_k}{}^{-1}\dot{\hat{W}}_{\bar{\sigma}_k} \tag{39}$$

Recall that:

$$\bar{\sigma}^T\left[\ \tilde{W}_{\bar{\sigma}}{}^{T}\bullet\ \xi_{\bar{\sigma}}(\bar{\sigma})\ \right]=\sum_{k=1}^{n}\tilde{W}_{\bar{\sigma}_k}{}^{T}\bullet\ \xi_{\bar{\sigma}_k}(\bar{\sigma})\ \bar{\sigma}_k \tag{40}$$

and choosing the learning law of RBFNNs as:

$$\dot{\hat{W}}_{\bar{\sigma}_k}=\Gamma_{\bar{\sigma}_k}\bullet\ \xi_{\bar{\sigma}_k}(\bar{\sigma})\ \bar{\sigma}_k \tag{41}$$

and substituting equations (40) and (41) into equation (39), $\dot{V}$ stays:

$$\dot{V}\le -K_{p\min}\left|\bar{\sigma}\right|^2+\bar{\sigma}^Td_v-\bar{\sigma}^T\left[\ W_{\bar{\sigma}}{}^{T}\bullet\ \xi_{\bar{\sigma}}(\bar{\sigma})\ \right] \tag{42}$$

where $K_{p\min}$ is the minimum singular value of K_p.

The $\dot{V}$ can be rewritten as:

$$\dot{V} \le -K_{p\min} |\bar{\sigma}|^2 + \left|\Delta f^T - P^T\right| |\bar{\sigma}| \tag{43}$$

with $P = \left[W_{\bar{\sigma}}{}^T \bullet \xi_{\bar{\sigma}}(\bar{\sigma}) \right]$ being the optimal compensation for $\Delta f = d_v$. According to the property of universal approximation of RBFNNs [Wang, 1996], there exists $\mu > 0$ satisfying $\left|\Delta f^T - P^T\right| \le \mu$, where μ is arbitrary and can be chosen as small as possible. Assuming that $\mu \le \beta |\bar{\sigma}|$ with $0 < \beta < 1$, one obtains that $\left|\Delta f^T - P^T\right| |\bar{\sigma}| \le \beta |\bar{\sigma}|^2 = \beta \bar{\sigma}^2$, therefore, $\dot{V}$ results in:

$$\dot{V} \le -\ K_{p\min} - \beta\ \bar{\sigma}^2 \tag{44}$$

Because of $K_{p\min} > \beta$, $\dot{V}$ is guaranteed negative definite.

4 SIMULATION RESULTS

In the simulations, the same kinematic model of the mobile robot described in [Sousa Jr. et al., 2002] is used. A reference trajectory was implemented and simulated using MATLAB/Simulink, which is a round rectangle trajectory generated by switching the reference linear and angular velocities in time,

$$v_{l_r} = \begin{cases} 0.785 \text{ m/s}, & (0+10n) \text{ s} < t \le (\pi + 10n) \text{ s} \\ 1.0 \text{ m/s}, & t > (\pi + 10n) \text{ s} \end{cases}$$

$$\omega_{a_r} = \begin{cases} 0.5 \text{ rad/s}, & (0+10n) \text{ s} < t \le (\pi + 10n) \text{ s} \\ 0.0 \text{ rad/s}, & t > (\pi + 10n) \text{ s} \end{cases}$$

where n, which changes from 0 to 3 step by step, is a positive constant. The initial posture of the reference trajectory is $[x_r, y_r, \theta_r]^T = [0, 1.6, 3\pi/2]^T$. The initial posture of the mobile robot is $[x_c, y_c, \theta]^T = [-1, 5, 3\pi/2]^T$.

To avoid impracticable control effort in transient period, the kinematic control signals are bounded by $|v_l| \le 9.5$ m/s and $|\omega_a| \le 3\pi/2$ rad/s, which represents the actuator saturation limits.

For this case, three types of control strategies are considered:

- Control 1: the proposed VSC without the discontinuous term, equation (35), that is, with $G = 0$;
- Control 2: the proposed VSC with the discontinuous term, equation (35), that is, with $G \neq 0$;
- Control 3: the VSC with NC, equations (37) and (41).

The gains for each simulation are summarized in the Table 1.

Table 1: Gains for the round rectangle trajectory.

Gains	Control 1	Control 2	Control 3
k_1	1.0	1.0	1.0
k_2	1.0	1.0	1.0
k_3	1.0	1.0	1.0
G_{11}	-	1.5	-
G_{22}	-	1.5	-
K_{p11}	1.5	1.5	1.5
K_{p22}	3.0	3.0	3.0
$\Gamma_{\sigma k}$	-	-	0.5

Moreover, in the Control 3, the number of hidden neurons used are 25. For simplicity, the centres of the localized Gaussian radial basis functions are evenly distributed in order to span the input space of the neural network, and the variance value is fixed at 3. The weights of the RBFNNs were initialized to zero, without to have any prior knowledge of the system disturbances. It is important to emphasize that different tracking performance can be achieved by adjusting parameters gains, and others factors, such as the size of the RBFNNs, centres and variances of Gaussian radial basis functions. Also, in the simulations, a bounded disturbance, $\rho_M(t)$ of equation (6), (see Figure 2), is applied to the kinematic model of the mobile robot, equation (4), which is given by [Canudas de Wit and Khennouf, 1995]:

$$\rho_M(t) = 1.45H\ \ t-9.0\ \ -1.45H\ \ t-40.0$$

where $H(\cdot)$ denotes the standard Heaviside step function.

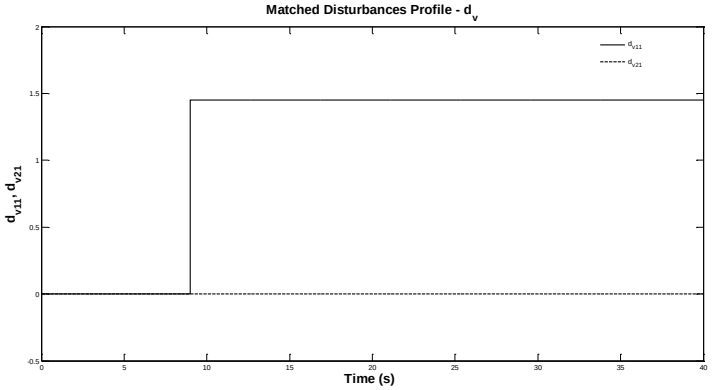

Figure 2: Disturbances applied in the mobile robot.

The results for Control 1 under the influence of disturbances are shown in Figures 3-10, where one can see that: the mobile robot can not track correctly the desired trajectory (Figures 3-6); there are nonzero tracking errors (Figure 7); the velocities tend to desired values (Figure 8), but they does not provide the control signals required to compensate the disturbances; the sliding surfaces does not converge to zero (Figure 9), although their derivatives converges (Figure 10).

The simulation results of the Control 2 are shown in Figures 11-18. The Figures 11-14 demonstrates that the controller seems to be able to drive the mobile robot to its desired posture and orientation. Although the tracking errors in Figure 15 tends to zero, it is achieved by performing vibrating control signals in the steady-state as shown in Figure 16, which is not realistic. Soon, in the Figure 17 the sliding surfaces converge to zero as well as their derivatives, but with chattering phenomenon as illustrated in Figure 18.

The Figures 19-27 illustrate the results for the Control 3. It is seem in Figures 19-22 that the mobile robot naturally describes a smooth path tracking over the reference trajectory. The tracking errors tends to zero as shown in Figure 23. Observe that in Figure 24 is demonstrated that there is no chattering in the linear and angular velocities, which represents the control signals. Both sliding surfaces (Figure 25) and their derivatives (Figure 26) converge to zero as well as the chattering is eliminated. The values of RBFNNs outputs presents behaviors similar to the disturbances (magnitudes in absolute values, see Figure 2) in the steady-state as shown in Figure 27, thus demonstrating the efficiency of the NC, (37) and (41).

5 CONCLUSIONS

A VSC and a VSC with NC considering disturbances in the kinematic model were proposed in this work, and used as an alternative solution to the trajectory tracking problem applied to nonholonomic mobile robot.

The VSC was considered because the invariance principle is applicable to it, but this technique exhibits the chattering phenomenon, that is highly undesirable. To avoid such a phenomenon, as well as to suppress the kinematic disturbances without having any prior knowledge of their boundary, RBFNNs were used in the replacement of the discontinuous portion of the classical VSC. Due to this replacement the invariance principle was no more verified, reducing the robustness, however the smooth control signal is achieved. The simulation results of the proposed approach were satisfactory.

As future works, it is validation of the AVSC and of the AVSC with NC in real-time applications of a nonholonomic mobile robot, as well as to realize the integration of torque controllers of the literature with these kinematic controllers proposed here.

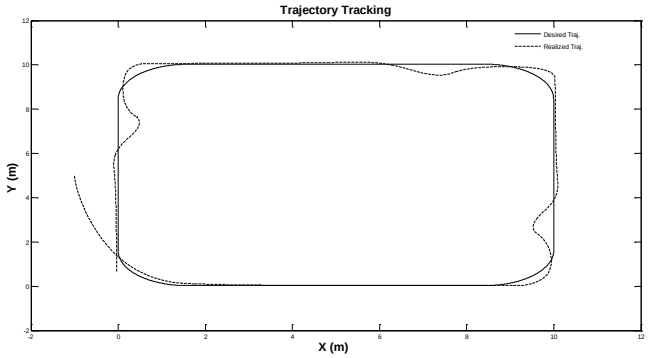

Figure 3: Reference trajectory and actual trajectory using Control 1.

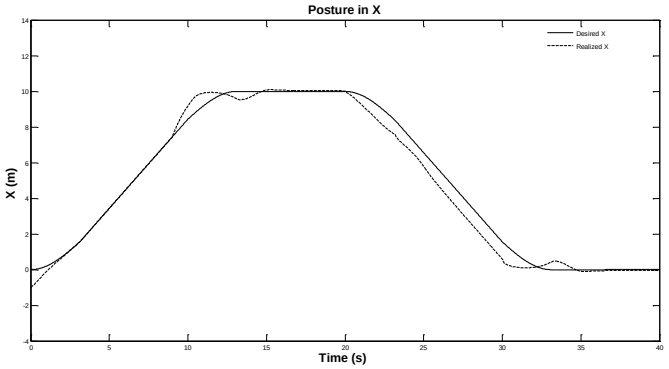

Figure 4: Desired posture x_r and realized posture x_c using Control 1.

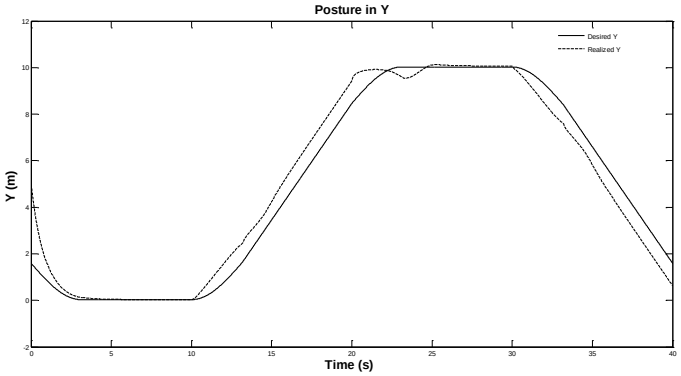

Figure 5: Desired posture y_r and realized posture y_c using Control 1.

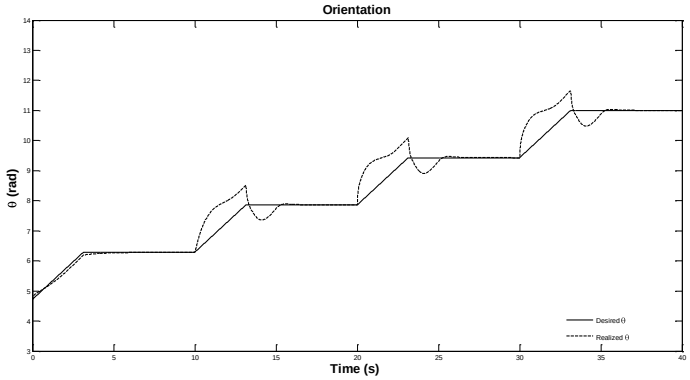

Figure 6: Desired orientation θ_r and realized orientation θ using Control 1.

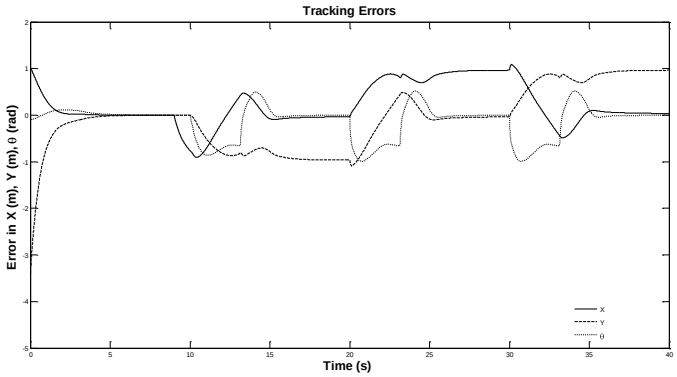

Figure 7: Tracking errors using Control 1.

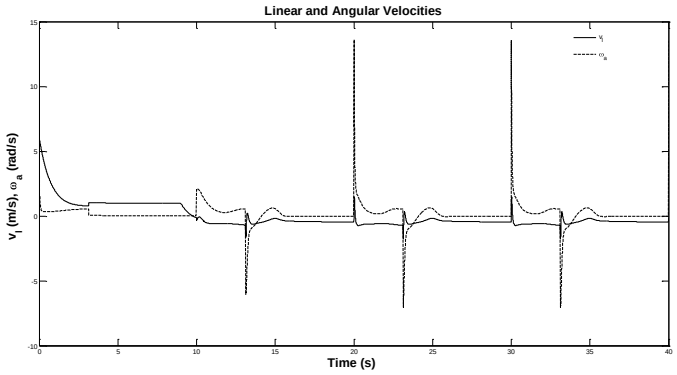

Figure 8: Linear and angular velocities of the mobile robot using Control 1.

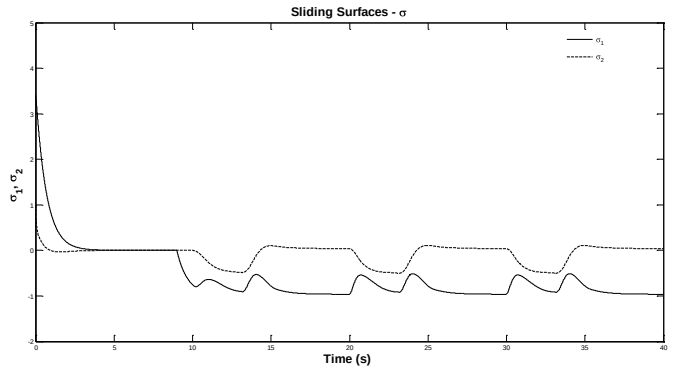

Figure 9: Sliding surfaces using Control 1.

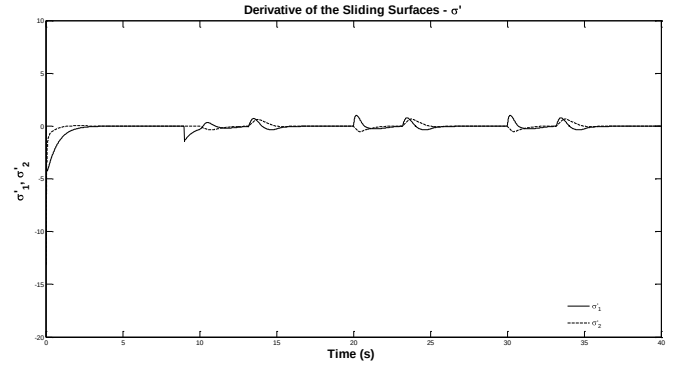

Figure 10: Derivative of the sliding surfaces using Control 1.

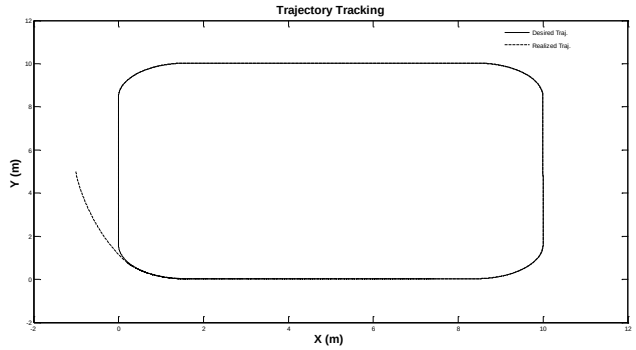

Figure 11: Reference trajectory and actual trajectory using Control 2.

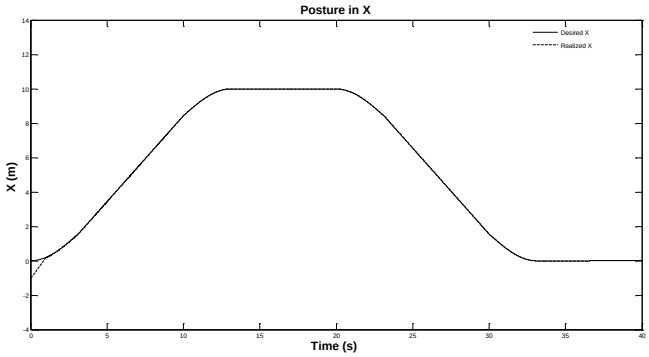

Figure 12: Desired posture x_r and realized posture x_c using Control 2.

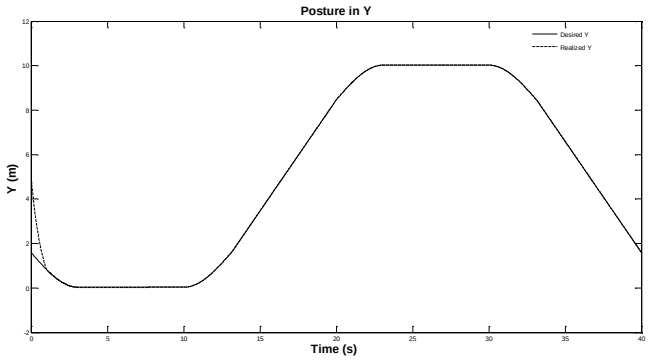

Figure 13: Desired posture y_r and realized posture y_c using Control 2.

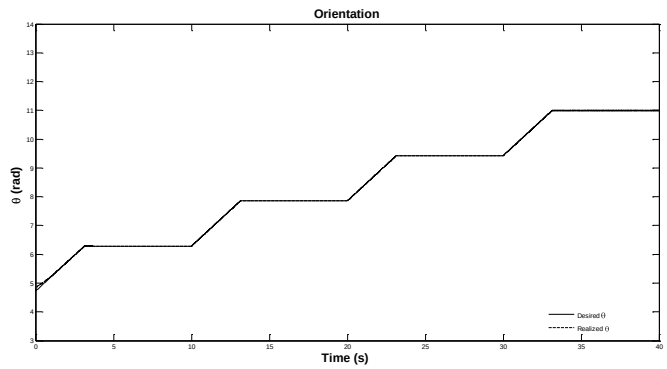

Figure 14: Desired orientation θ_r and realized orientation θ using Control 2.

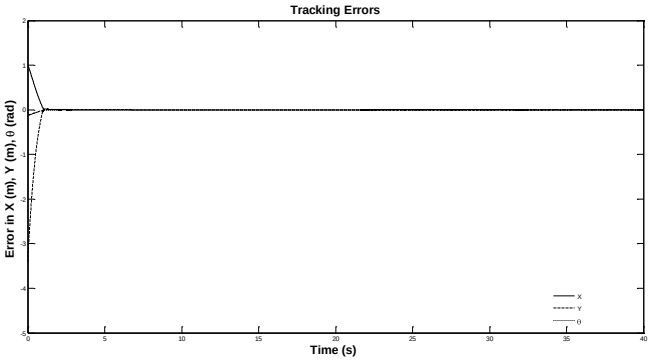

Figure 15: Tracking errors using Control 2.

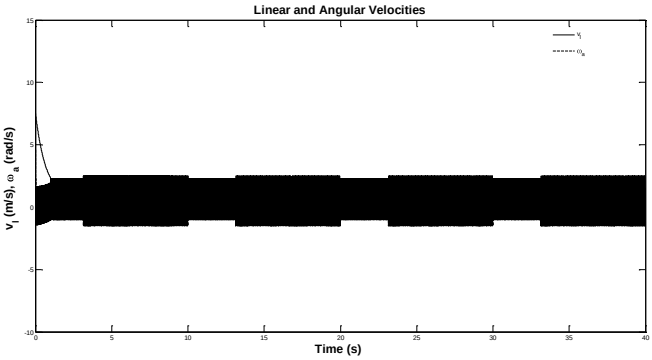

Figure 16: Linear and angular velocities of the mobile robot using Control 2.

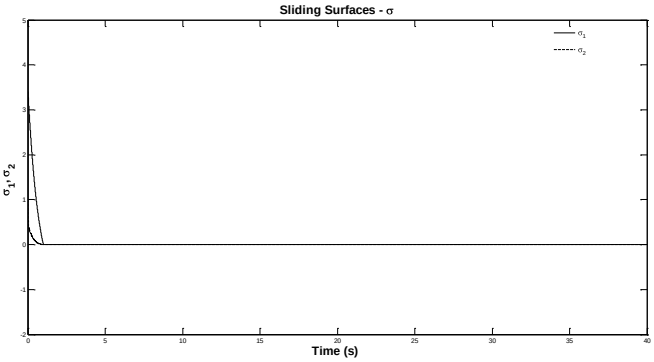

Figure 17: Sliding surfaces using Control 2.

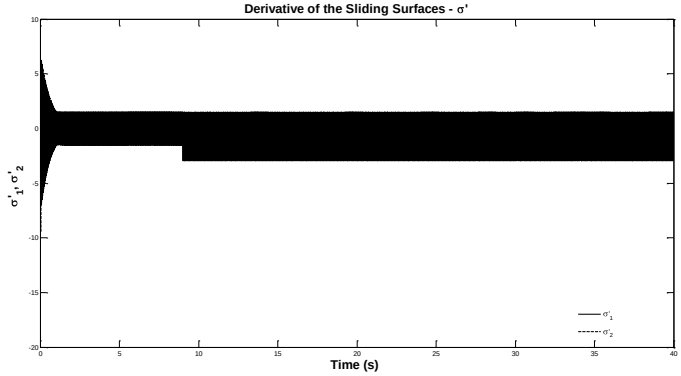

Figure 18: Derivative of the sliding surfaces using Control 2.

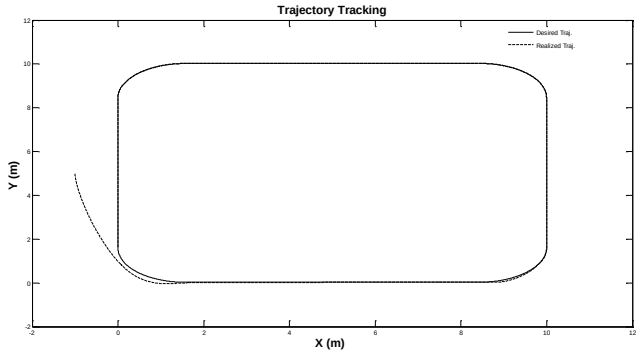

Figure 19: Reference trajectory and actual trajectory using Control 3.

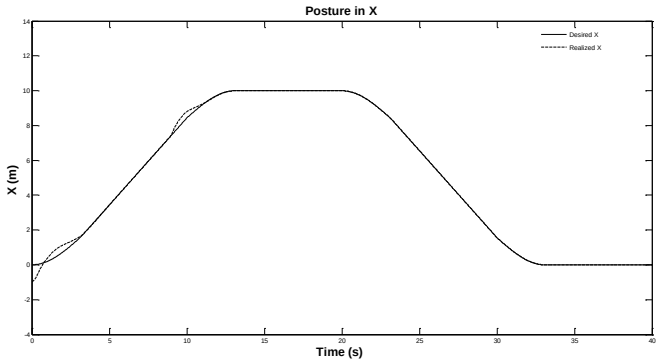

Figure 20: Desired posture x_r and realized posture x_c using Control 3.

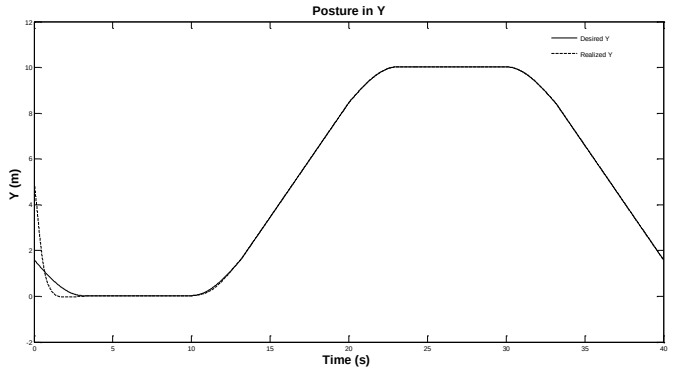

Figure 21: Desired posture y_r and realized posture y_c using Control 3.

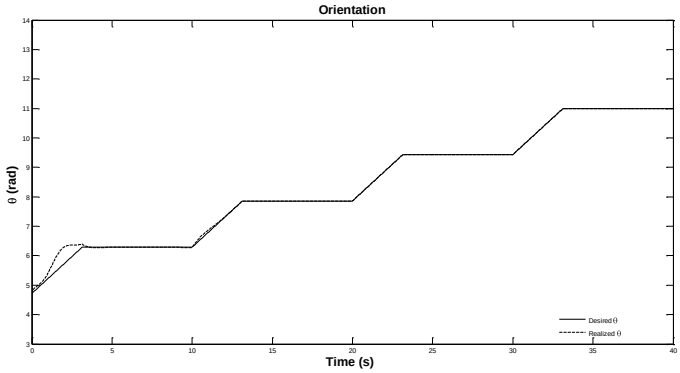

Figure 22: Desired orientation θ_r and realized orientation θ using Control 3.

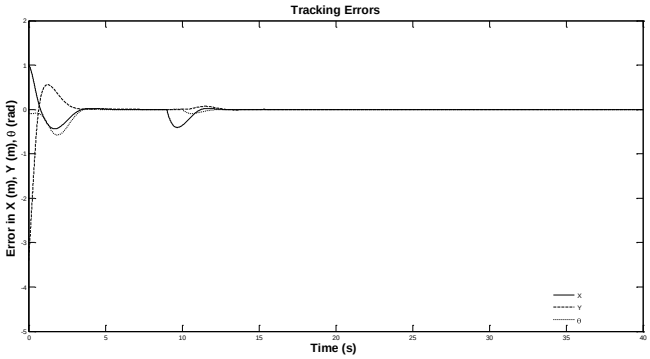

Figure 23: Tracking errors using Control 3.

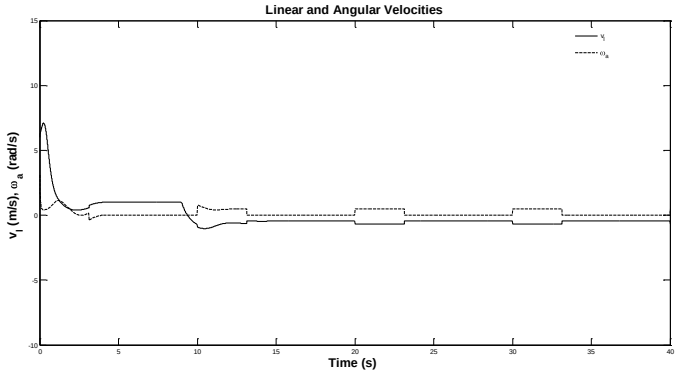

Figure 24: Linear and angular velocities of the mobile robot using Control 3.

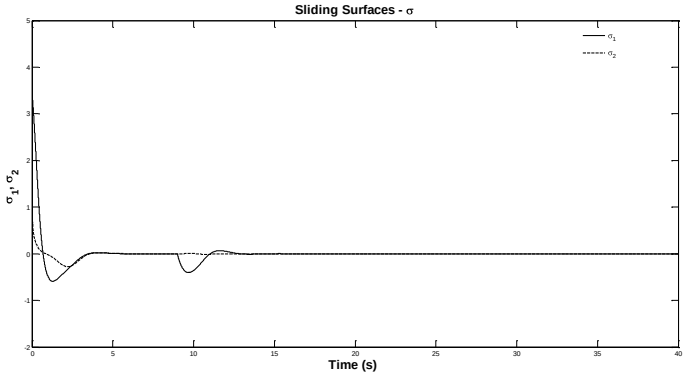

Figure 25: Sliding surfaces using Control 3.

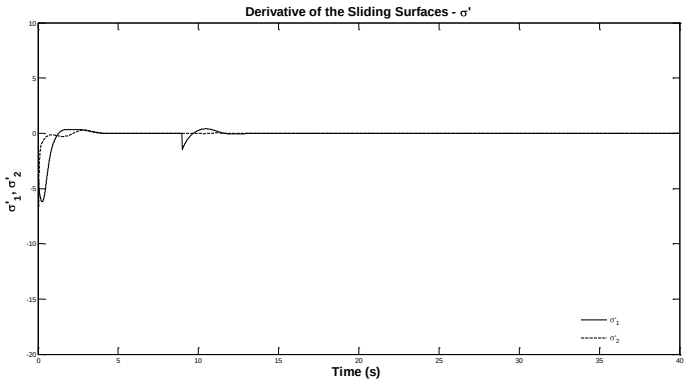

Figure 26: Derivative of the sliding surfaces using Control 3.

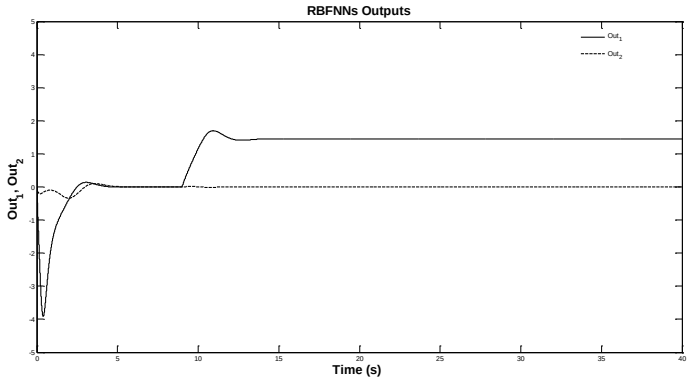

Figure 27: RBFNNs Outputs of the Control 3.

6 ACKNOWLEDGEMENTS

The authors would like to acknowledge the CNPq by the financial support.

7 REFERENCES

Campion, G. and Chung, W. (2008). Wheeled Robots. *Handbook of Robotics*, Springer-Verlag: Berlin, Heidelberg, Germany, pp. 391-410.

Morin, P. and Samson, C. (2008). Motion Control of Wheeled Mobile Robots. *Handbook of Robotics*, Springer-Verlag: Berlin, Heidelberg, Germany, pp. 799-826.

Utkin, V., Guldner, J. and Shi, J. (2009). *Sliding Mode Control in Eletro-Mechanical Systems*. Second Edition, CRC Press, Taylor & Francis Group, Boca Raton, Florida, USA.

Decarlo, R. A., Zak, S. H. and Drakunov, S. (1996). Variable Structure Sliding Mode Controller Design. *The Control Handbook*, CRC Press: Boca Raton, FL, pp. 941-951.

Hung, J. Y., Gao, W. and Hung, J. C. (1993). Variable Structure Control: A Survey. *IEEE Trans. Industrial Electronics*, vol. 40, Iss. 1, pp. 2-22.

Gao, W. and Hung, J. C. (1993). Variable Structure Control of Nonlinear Systems: A New Approach. *IEEE Trans. Industrial Electronics*, Vol. 40, Nº. 1, pp. 45-55.

Shuwen, P., Hongye, S., Xiehe, H. and Jian, C. (2000). Variable Structure Control Theory and Application: A Survey. *Proc. World Congress Intel. Control and Automation*, pp. 2977-2981.

Efe, M. O. and Kaynak, O. (2001). Variable Structure Systems Theory based Training Strategies for Computationally Intelligent Systems. *Proc. Annual Conference IEEE Industrial Electronics Society*, pp. 1563-1576.

Kaynak, O., Erbatur, K. and Ertugrul, M. (2001). The Fusion of Computationally Intelligent Methodologies and Sliding Mode Control - A Survey. *IEEE Trans. Industrial Electronics*, vol. 48, Iss. 1, pp. 4-17.

Seshagiri, S., and Khalil, H. K. (2000). Output Feedback Control of Nonlinear Systems using RBF Neural Networks. *IEEE Trans. Neural Networks*, vol. 11, Iss. 1, pp. 69-79.

Elyoussef, E. S., Martins, N. A., Bertol, D. W., Pieri, E. R., and Jungers, M. (2010). On a Wheeled Mobile Robot Trajectory Tracking Control: 1st and 2nd Order Sliding Modes Applied to a Compensated Inverse Dynamics. *Proceedings of the 11th Pan-American Congress of Applied Mechanics - PACAM XI*.

Li, Y., Zhu, L., Wang, Z. and Liu, T. (2009). Trajectory Tracking for Nonholonomic Wheeled Mobile Robots based on an Improved Sliding Mode Control Method. *Proc. International Colloquium on Computing, Communication, Control, and Management*, vol. 2, pp. 55-58.

Lee, J. H., Lin, C., Lim, H. and Lee, J. M. (2009). Sliding Mode Control for Trajectory Tracking of Mobile Robot in the RFID Sensor Space. *International Journal of Control, Automation, and Systems*, vol. 7, Iss. 3, pp. 429-436.

Defoort, M., Palos, J., Floquet, T., Kokosy, A., Perruquetti, W. (2007). Practical Stabilization and Tracking of a Wheeled Mobile Robot with Integral Sliding Mode Controller. *Proceedings of the 46th IEEE Conference on Decision and Control*, pp. 1999-2004.

Chwa, D. (2004). Sliding-Mode Tracking Control of Nonholonomic Wheeled Mobile Robots in Polar Coordinates. *IEEE Transactions on Control Systems Technology*, vol. 12, Iss. 4, pp. 637- 644.

Chwa, D., Seo, J. H., Kim, P. and Choi, J. Y. (2002). Sliding Mode Tracking Control of Nonholonomic Wheeled Mobile Robots. *Proceedings of the 2002 American Control Conference*, vol. 5, pp. 3991-3996.

Yang, J.-M. and Kim, J.-H. (1999). Sliding Mode Control for Trajectory Tracking of Nonholonomic Wheeled Mobile Robots. *IEEE Trans. Robotics and Automation*, vol. 15, Iss. 3, pp. 578-587.

Yang, J.-M. and Kim, J.-H. (1999a). Sliding Mode Motion Control of Nonholonomic Mobile Robots. *IEEE Control Systems Magazine*, vol. 19, Iss. 2, pp. 15-23.

Shim, H.-S., Kim, J.-H. and Koh, K. (1995). Variable Structure Control of Nonholonomic Wheeled Mobile Robot. *Proc. 1995 IEEE International Conference on Robotics and Automation*, vol. 2, pp. 1694-1699.

Guldner, J. and Utkin, V. I. (1994). Stabilization of Nonholonomic Mobile Robots using Lyapunov Functions for Navigation and Sliding Mode Control. *Proc. of the 33rd IEEE Conference on Decision and Control*, vol. 3, pp. 2967-2972.

Canudas de Wit, C. and Khennouf, H. (1995). Quasi-Continuous Stabilizing Controllers for Nonholonomic Systems: Design and Robustness Considerations. *Proceedings of the 3rd European Control Conference*, pp. 2630-2635.

Martins, N. A. and De Pieri, E. R. (2010). Trajectory Tracking of a Nonholonomic Mobile Robot with Kinematic Uncertainties and Disturbances: An Adaptive Variable Structure Controller. To appear in *Proceedings of the 4th Workshop in Applied Robotics and Automation - ROBOCONTROL'2010*.

DeCarlo, R.A., Stanislaw, H..Z. and Mathews, G.P. (1988). Variable Structure Control of Nonlinear Multivariable Systems: A Tutorial, *Proceedings of the IEEE*, vol. 76, Iss. 3, pp. 212-232.

Martins, N. A., Bertol, D. W., Lombardi, W. C., De Pieri, E. R. and Castelan, E. B. (2008). Trajectory Tracking of a Nonholonomic Mobile Robot with Parametric and Nonparametric Uncertainties: A Proposed Neural Control. *International Journal of Factory Automation, Robotics and Soft Computing*, vol. 2, pp. 103-110.

Ge, S. S. (1996). Robust Adaptive NN Feedback Linearization Control of Nonlinear Systems. *Int. J. Systems Science*, pp. 1327-338.

Wang, L. X. (1996). *A Course in Fuzzy Systems and Control*. Prentice-Hall, Inc., Upper Saddle River, NJ, USA.

Sousa Jr., C., Hemerly, E. M. and Galvao, R. K. H. (2002). Adaptive Control for Mobile Robot using Wavelet Networks. *IEEE Trans. on Systems, Man, and Cybernetics, Part B*, vol. 32, Iss. 4, pp. 493-504.